Adsorption of Mixtures Containing Subcritical Fluids on Activated Carbon

D. D. Do and H. D. Do
Dept. of Chemical Engineering, University of Queensland, St. Lucia, Qld 4072, Australia

A theoretical analysis of adsorption of mixtures containing subcritical adsorbates into activated carbon is presented as an extension to the theory for pure component developed earlier by Do and coworkers. In this theory, adsorption of mixtures in a pore follows a two-stage process, similar to that for pure component systems. The first stage is the layering of molecules on the surface, with the behavior of the second and higher layers resembling to that of vapor–liquid equilibrium. The second stage is the pore-filling process when the remaining pore width is small enough and the pressure is high enough to promote the pore filling with liquid mixture having the same compositions as those of the outermost molecular layer just prior to pore filling. The Kelvin equation is applied for mixtures, with the vapor pressure term being replaced by the equilibrium pressure at the compositions of the outermost layer of the liquid film. Simulations are detailed to illustrate the effects of various parameters, and the theory is tested with a number of experimental data on mixture. The predictions were very satisfactory.

Introduction

Characterization of a porous solid in order to understand the adsorption and desorption phenomena is one of the most important problems in separation and purification of gases and vapors. In either purification or separation, the need to know the equilibrium competition between adsorbing species is essential for the proper design of the adsorption column (Ruthven, 1984; Yang, 1987; Do, 1998a). Experimental data of mixtures are very scarce in the literature. Table 1 summarizes the various theoretical models available in the literature, and the various experimental studies on mixtures involving subcritical adsorbates. The principal reason for the scarce information on mixture adsorption data is perhaps the large number of combinations to be explored for mixtures. To deal with this problem, there are two options. Either an experimental program has to be set up to study the specific problem at hand, and even with this the combination of various parameters can be large, or a theory for mixtures that uses pure component data is applied to predict the adsorption isotherm for the mixture. There are two points that must be addressed concerning use of the latter approach. First the theory must reasonably describe the mixture data, and that should help reduce the amount of data needed, and secondly, since particle properties such as the pore-size distribution affect the equilibria, the model should be able to account for this in the prediction of adsorption isotherm.

Concerning pure component adsorption equilibria, it is in the literature that the pore-size distribution strongly affects the adsorption capacity, and this has prompted many investigations to address this problem. Different analysis tools, such as the classic method, potential energy method, the DFT method, and the molecular simulation method, have been used. And since PSD affects the adsorptive capacity of different species in different ways, we would expect that it affects the competitive adsorption equilibria for mixtures.

Unfortunately, the effect of PSD on adsorption equilibria for mixtures is not well reported in the literature. There have been some attempts using various tools to address this problem, but the problem is not completely solved. Nguyen and Do (2001) recently studied the effect of pore-size distribution on the competitive adsorption of supercritical fluids. In this article, we address the effect of PSD on the competitive adsorption of subcritical fluids in a porous carbon medium. This work is an extension of the previous work of Do and cowork-

Correspondence concerning this article should be addressed to D. D. Do.

Table 1. Literature on Various Approaches in Dealing With Adsorption of Mixtures

Ref.	Approach
Lewis et al. (1950)	Lewis rule
Cook and Basmadjian (1965)	Graphical method for binary
Myers and Prausnitz (1965); LeVan and Vermeulen (1981); O'Brien and Myers (1985); Myers and Valenzuela (1986); Tien (1986); Talu and Zwiebel(1986); Moon and Tien (1987, 1988); O'Brien and Myers (1988); Myers (1989); Richter et al. (1989); Karavias and Myers (1992); Frey and Rodrigues (1994); Sircar (1995); Yun et al., (1996)	IAST approach, its extension and applications
Sircar and Myers (1973)	Surface potential model
Suwanayuen and Danner (1980); Talu and Kabel (1987); Talu and Myers (1988a,b)	Vacancy solution model
Grant and Manes (1966); Mehta and Danner (1985); Sundaram (1995); Shapiro and Stenby (1998)	Potential theory approach
Ruthven and Wong (1985); Liedy and Schlunder (1988)	Statistical model
Hoory and Prausnitz (1967); Zhou et al. (1994); Zheng and Gu (1998)	Equation of state
Dunne and Myers (1994); Frances et al. (1995); Sircar (1995)	Study on the effect of adsorbate size
Russell and LeVan (1996)	Group contribution theory
Myers and Sircar (1972); Sircar (1985); Talu and Myers (1988); Rudisill and LeVan (1988); Sircar (1991a); Staudt et al. (1996, 1998); Rao and Sircar (1999)	Thermodynamics approach
Valenzuela and Myers (1988); Sircar (1991b); Koopal et al. (1994)	Heterogeneity

ers on pure component adsorption in carbon media (Do, 1998b; Nguyen and Do, 1999; Do et al., 2001; Do and Do, 2002). The competition for adsorption by different species on the surface would depend on many factors, such as the heat of adsorption, which is enhanced by the overlapping of potential fields put out by the two opposite walls of slitlike micropores, and the heat of vaporization from molecular layers above the first layer. Since the heat of vaporization is different from layer to layer, due to the different compositions in each layer, information on the liquid–vapor equilibrium is needed in this modeling approach. This is what we address in this article. Here we extend the layering procedure of Hill (1946), who developed equations for mixtures adsorbing on a flat surface, to porous media with a pore-size distribution (PSD). The distinct differences between a flat surface and a porous medium are the PSD and the enhancement in adsorption in small pores.

Theoretical Development

The method presented in this article is an extension of the work developed earlier by Do and coworkers (Do, 1998b; Nguyen and Do, 1999; Do et al., 2001), who proposed a new model for adsorption of pure component in activated carbon. Pore-size distribution is taken into account, and it has a strong effect on the adsorption equilibria, where the enhancement in adsorption is very significant in small pores that typically have a dimension of one to two times the collision diameter. Adsorption in any pore is treated as a sequence of two steps: layering of molecules on surfaces followed by a pore-filling step. The layering process is enhanced in small pores. The same principles are now applied here for mixture adsorption. To achieve this we need to establish the appropriate equation for the calculation of the layer thickness as well as the amount adsorbed for each species in the adsorbed layer. But first we will present briefly the potential energy equation that we use to calculate the enhancement of adsorption for different species.

Potential energy

In general the density inside a pore is much higher than that in the bulk fluid phase. This is due to the attractive forces between the pore surface atoms and the adsorbate molecules. Long-range attraction can result in greater pressure exerted by occluded molecules than that exerted by molecules in the bulk fluid phase. Only when the size of the pore is large enough (usually of the order of 5 or greater than the collision diameter, σ_{sf}) the pressure within the pore is the same as the bulk fluid pressure. This means that both the adsorbed molecules and the occluded molecules are enhanced by the interactive forces. If these forces are dispersive, the potential energy of interaction between an adsorbate molecule i with the surface atom j can be calculated by the 12–6 Lennard-Jones potential energy equation (Eq. 1)

$$\varphi_{ij} = 4\epsilon_{ij}\left[\left(\frac{\sigma_{ij}}{r_{ij}}\right)^{12} - \left(\frac{\sigma_{ij}}{r_{ij}}\right)^{6}\right] \tag{1}$$

If the interaction is assumed to be purely an additive, one can sum up all the pairwise potential energies (Eq. 1) between the molecule and all the surface atoms, including those lying underneath the outermost surface layers. Here r_{ij} is the distance between the molecule i and the surface atom j. The parameters ϵ_{ij} and σ_{ij} are calculated from known molecular properties ϵ_{ij}, ϵ_{jj}, σ_{ii}, σ_{jj} using the Lorentz–Betherlot rule. If the distance of the adsorbate molecule from the surface is much greater than the distance between two adjacent carbon atom centers, the process of summation of 12–6 Lennard-Jones potential energy can be approximated by an integration. In carbonaceous materials, surfaces are usually formed with layers of graphite separated by the distance Δ. Steele's well-known 10–4–3 potential energy equation for a molecule of species k at distance z from the center of the outermost

carbon layer of one wall can describe this situation

$$\varphi_k(z) = \varphi_{k,w}\left[\frac{1}{5}\left(\frac{\sigma_{ks}}{z}\right)^{10} - \frac{1}{2}\left(\frac{\sigma_{ks}}{z}\right)^{4} - \frac{\sigma_{ks}^4}{6\Delta(z+0.61\Delta)^3}\right] \tag{2}$$

where $\varphi_{k,w} = 4\pi\rho_s\sigma_{ks}^2\Delta\epsilon_{ks}$. For a carbon surface modeled as layers of graphite sheets the following values are usually used, $\rho_s = 114\times10^{-27}$ m^{-3}, $\Delta = 3.354\times10^{-10}$ m, $\sigma_{ss} = 3.4 \times 10^{-10}$ m, $(\epsilon_{ss}/k_B) = 28$ K. For a slit pore having two walls separated by a distance H, the potential energy equation between an adsorbate molecule of species k and the pore is

$$\varphi_{P,k} = \varphi_k(z) + \varphi_k(H - z) \tag{3}$$

Here the distance z is taken as the minimum distance from the center of the adsorbate molecule to the plane passing through all the carbon centers of the outermost layer. This equation allows us to obtain a distribution of the potential energy in terms of distance from the pore surface for all species k concerned. The bulk fluid phase is taken as the reference of zero potential energy.

Layering adsorption mechanism

The adsorption energy in a pore is always greater than that of a flat surface with the same surface chemistry. What this means is that if the fluid pressure inside a pore is P_p (which is different from the bulk fluid pressure) and the fluid is subcritical, the adsorption process in a pore is viewed as that of molecular layering, a process akin to that postulated by BET. The key difference here is the enhancement in the adsorption due to the higher heat of adsorption and higher pore pressure than the bulk fluid pressure. BET was used by Do and coworkers (Do, 1998b; Do et al., 2001) as the equation to describe the layering for pure component adsorption in pores of all dimensions. The situation is complex for mixtures, because different species adsorbed differently in each layer due to their difference in adsorption affinities as well as the difference in compositions. Furthermore the enhancement in small pores is also different from species to species. The adsorption of a particular species on the bare surface depends on the adsorption energy, which is greater in smaller pores due to the enhancement. We shall restrict ourselves to binary mixtures in this article. The adsorption process for creating a second and higher layer is assumed to follow that of vapor–liquid equilibrium.

Notation Used. To help with the clarity of the modeling, we first introduce the notation used in the theoretical model. The molar adsorption heat involved in the adsorption of molecule A on a layer containing x_A mole fraction of A is denoted as

$$Q_A(x_A, x_B) \qquad \text{(J/mol)} \tag{4a}$$

Similarly, the molar adsorption heat involved in the adsorption of molecule B on the same layer is

$$Q_B(x_A, x_B) \qquad \text{(J/mol)} \tag{4b}$$

This means that the adsorption heats involved in the adsorption of A on a layer of pure A and a layer of pure B are $Q_A(1,0)$ and $Q_A(0,1)$, respectively. Similarly the adsorption heats involved in the adsorption of B on a layer of pure A and a layer of pure B are $Q_B(1,0)$ and $Q_B(0,1)$, respectively. Note that $Q_A(1,0)$ and $Q_B(0,1)$ are the heats of vaporization of pure liquid A and liquid B (λ_A and λ_B), respectively.

Using the same terminology, the heat of adsorption involved in the adsorption of A and B on a bare surface within a pore is denoted as Q_{A0} and Q_{B0}. Due to the enhancement of adsorption in small pores, the heats of adsorption on a bare surface are a function of pore size. In general, the smaller the pore, the greater the adsorption heat. Therefore, we assign the following notation for the heats of adsorption on a bare surface

$$Q_{A0}(H) \qquad \text{and} \qquad Q_{B0}(H) \tag{5}$$

Here the subscript 0 denotes the bare surface. When H is very large, the preceding two heats approach the heats of adsorption on a flat surface, which are obtained from the BET analysis of data of a nonporous surface such as graphitized carbon black. We shall assume that the adsorption heats involved in the second and higher layers are not affected by the pore size.

Consider a surface covered with various layers of molecules (Figure 1). The area covered by a stack of j molecules is denoted by S_j. The adsorption of molecule A on the $(i-1)$-th layer has an adsorption heat of $Q_A(x_{A,i-1}, x_{B,i-1})$, which is a function of just the mole fractions of the $(i-1)$-th layer, and not on the compositions of the layers lying underneath, that is, it is independent of the compositions of the underneath layers. Similarly, the adsorption of molecule B on the $(i-1)$-th layer has an adsorption heat of $Q_B(x_{A,i-1}, x_{B,i-1})$. Let us now consider the rates of adsorption and desorption on the first layer, and the subsequent layers.

Adsorption on the First Layer. The rates of adsorption of molecule A on a bare surface and desorption from the sec-

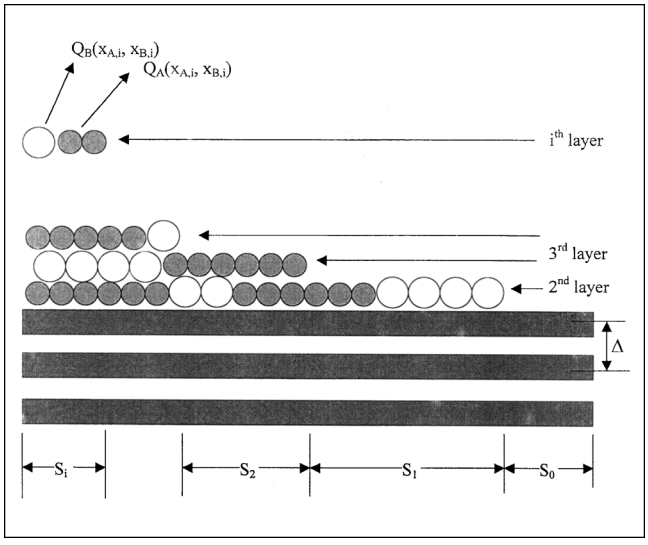

Figure 1. Adsorption layering on a surface.

tion containing one layer of molecules are

$$r_{\text{ads}} = k_{A,a} S_0 p_A \tag{6a}$$

$$r_{\text{des}} = k_{A,d} S_1 x_{A,1} \exp\left[-\frac{Q_{A0}(H)}{RT} \right] \tag{6b}$$

where $x_{A,1}$ is the mole fraction of A in the first layer. At equilibrium these two rates are equal, and this gives

$$\left(\frac{k_{A,d}}{k_{A,a}} \right)_{\text{surface}} = \frac{S_0 p_A}{S_1 x_{A,1}} \exp\left[\frac{Q_{A0}(H)}{RT} \right] \tag{7}$$

But based on the evaporation and condensation from a pure liquid A (Appendix 1), we have

$$\frac{k_{A,d}}{k_{A,a}} = p_A^0 \exp\left[\frac{Q_A(1,0)}{RT} \right] \tag{8}$$

where p_A^0 is the vapor pressure of A and $Q_A(1,0)$ is the heat of vaporization of A, λ_A. We shall assume that the ratio of the rate constants for condensation and evaporation from a pure liquid A is the same as the ratio of the rate constants for adsorption onto a bare surface and desorption from the first adsorbed layer. Thus, by equating Eqs. 7 and 8, we get the following relationship between the mole fraction and surface areas

$$S_1 x_{A,1} = S_0 \left(\frac{p_A}{p_A^0} \right) \exp\left[\frac{Q_{A0}(H) - Q_A(1,0)}{RT} \right] \tag{9}$$

Similarly following the same procedure for molecule B, we obtain

$$S_1 (1 - x_{A,1}) = S_0 \left(\frac{p_B}{p_B^0} \right) \exp\left[\frac{Q_{B0}(H) - Q_B(0,1)}{RT} \right] \tag{10}$$

where $Q_B(0,1)$ is the heat of vaporization of B, λ_B. The exponential terms in the preceding two equations are the BET constant C's for species A and B in pore of width H. These constants are enhanced due to the overlapping of the potential fields exerted by the two opposite walls. They are related to the BET constants of a corresponding flat surface as follows

$$C_A(H) = \exp\left[\frac{Q_{A0}(H) - Q_A(1,0)}{RT} \right] = C_{A,\text{flat}} \exp\left[\frac{Q_{A0}(H) - Q_{A0}(\infty)}{RT} \right] \tag{11b}$$

$$C_B(H) = \exp\left[\frac{Q_{B0}(H) - Q_B(0,1)}{RT} \right] = C_{B,\text{flat}} \exp\left[\frac{Q_{B0}(H) - Q_{B0}(\infty)}{RT} \right] \tag{11b}$$

Thus, if we know the BET constants for a flat surface for species A and B, the BET constants for a pore of width H can be calculated from Eqs. 11. The adsorption heats $Q_{A0}(H)$ and $Q_{A0}(\infty)$ are estimated as the depths of the potential energy profiles for a pore width, H, and for a flat surface (Do et al., 2001).

Thus, combining Eqs. 11 with Eqs. 9 and 10, we have the following relationship between the mole fraction of the first layer, the surface areas, and pressures p_A and p_B

$$S_1 x_{A,1} = S_0 \left(\frac{p_A}{p_A^0} \right) C_A(H) \tag{12a}$$

$$S_1 (1 - x_{A,1}) = S_0 \left(\frac{p_B}{p_B^0} \right) C_B(H) \tag{12b}$$

It is noted that the pressures p_A and p_B are the pressures inside a pore, and are different from their corresponding pressures in the bulk gas phase, which is due to enhancement. We shall discuss this enhancement in pressure later in the subsection on the pore pressure.

Adsorption of the Second and Higher Layers. At equilibrium, the rate of adsorption of molecule A onto the $(i-1)$-th layer is equal to the rate of desorption from the ith layer, that is,

$$k_{A,a} S_{i-1} p_A = k_{A,d} S_i x_{A,i} \exp\left[-\frac{Q_A(x_{A,i-1}, x_{B,i-1})}{RT} \right] \tag{13}$$

for $i = 2, 3, \ldots, n$. Making use of the condensation and evaporation from pure liquid A (Eq. 8), the preceding equation can be rewritten as

$$S_i x_{A,i} = S_{i-1} \left(\frac{p_A}{p_A^0} \right) \exp\left[\frac{Q_A(x_{A,i-1}, x_{B,i-1}) - Q_A(1,0)}{RT} \right] \tag{14a}$$

Similarly the corresponding equation for species B is

$$S_i (1 - x_{A,i}) = S_{i-1} \left(\frac{p_B}{p_B^0} \right) \exp\left[\frac{Q_B(x_{A,i-1}, x_{B,i-1}) - Q_B(0,1)}{RT} \right] \tag{14b}$$

But from the vapor–liquid equilibrium for mixtures of A and B (Appendix B), the exponential factors in the preceding equations can be obtained from the information of vapor–liquid equilibrium. Letting

$$\exp\left[\frac{Q_A(x_{A,i-1}, x_{B,i-1}) - Q_A(1,0)}{RT} \right] = f_A(x_{A,i-1}, x_{B,i-1}) \tag{15a}$$

$$\exp\left[\frac{Q_B(x_{A,i-1}, x_{B,i-1}) - Q_B(0,1)}{RT} \right] = f_B(x_{A,i-1}, x_{B,i-1}) \tag{15b}$$

which are known functions of mole fractions, Eqs. 14 can be simplified as

$$S_i x_{A,i} = S_{i-1}\left(\frac{p_A}{p_A^0}\right) f_A(x_{A,i-1}, x_{B,i-1}) \tag{16a}$$

$$S_i(1-x_{A,i}) = S_{i-1}\left(\frac{p_B}{p_B^0}\right) f_B(x_{A,i-1}, x_{B,i-1}) \tag{16b}$$

The set of equations (Eqs. 12 and 16) completely define the mole fractions in all layers, and the surface areas S_j ($j = 1, 2, \ldots, n$) in terms of S_0.

Solutions for the Mole Fractions and the Areas Occupied by i Layers. Solving the set of equations (Eqs. 12 and 16), the solutions for the mole fractions for all layers are

$$x_{A,1} = \frac{C_A(H)\left(p_A/p_A^0\right)}{E_1} \tag{17a}$$

$$x_{A,i} = \frac{\left(p_A/p_A^0\right) f_A(x_{A,i-1})}{E_i} \tag{17b}$$

for $i = 2, 3, \ldots, n$. Here the function E_1 is a function of partial pressures p_A and p_B, and the vertical interaction between adsorbate and adsorbent, which is characterized by the BET constants $C_A(H)$ and $C_B(H)$. It is given by

$$E_1 = C_A(H)\left(\frac{p_A}{p_A^0}\right) + C_B(H)\left(\frac{p_B}{p_B^0}\right) \tag{18a}$$

The function E_i (for $i = 2, 3, \ldots$) depends on partial pressures p_A and p_B, and the characteristics of the vapor–liquid equilibrium with the liquid having compositions of the ith layer. It is given by

$$E_i = \left(\frac{p_A}{p_A^0}\right) f_A(x_{A,i-1}) + \left(\frac{p_B}{p_B^0}\right) f_B(x_{A,i-1}) \tag{18b}$$

Equations 17 are recurrence equations. Mole fractions of the first layer can be calculated from Eq. 17a, and once these are known, the functional form for vapor–liquid equilibrium $f_A(x_{A,1})$ and $f_B(x_{A,1})$ can be evaluated. Therefore E_2 can be calculated from Eq. 18b, and, thence, the mole fraction $x_{A,2}$ of the second layer can be calculated from Eq. 17b. The same procedure is then used to calculate the mole fractions of the higher layers using Eqs. 18b and 17b. It should be emphasized that the mole fraction is distributed across the adsorption layer. This is in contrast to other macroscopic models for mixture adsorption in the literature, where the uniform concentration in the adsorbed phase was assumed.

Solution of the equation set (Eqs. 12 and 16) also gives the solutions for the surface area S_i, on which there are i layers of molecules. These solutions are written in terms of S_0, as given below

$$S_1 = S_0 E_1 \tag{19a}$$

$$S_i = S_0 E_1 E_2 \cdots E_{i-1} E_i \tag{19b}$$

Average Thickness of the Adsorbed Layer. We have obtained the mole fractions and the areas occupied by the i layers. Now we use these to calculate the average thickness of the adsorbed layer and the amounts adsorbed by species A and B. Let $t_{A,m}$ be the thickness of the monolayer of pure A, and $t_{B,m}$ be that of pure B. Since different species have different sizes (or liquid molar volumes), the fraction area of the layer i occupied by the species A is not necessarily the same as the mole fraction $x_{A,i}$ of that layer. We denote this fraction as $\alpha_{A,i}$, and it can be approximated by (Hill, 1946)

$$\alpha_{A,i} = \frac{x_{A,i}}{x_{A,i} + (1-x_{A,i})\left(v_{B,M}/v_{A,M}\right)^{2/3}} \tag{20}$$

where v_M is the liquid molar volume. The volume occupied by the species A and B in the first layer are

$$(S_1 + S_2 + \cdots + S_n)\,\alpha_{A,1} t_{A,m} \tag{21a}$$

and

$$(S_1 + S_2 + \cdots + S_n)(1-\alpha_{A,1}) t_{B,m} \tag{21b}$$

Thus, the total volume occupied by the first layer is

$$(S_1 + S_2 + \cdots + S_n)\left[\alpha_{A,1} t_{A,m} + (1-\alpha_{A,1}) t_{B,m}\right] \tag{22}$$

Similarly the total volume occupied by the second layer is

$$(S_2 + S_3 + \cdots + S_n)\left[\alpha_{A,2} t_{A,m} + (1-\alpha_{A,2}) t_{B,m}\right] \tag{23}$$

and so on, and the total volume occupied by the nth layer is

$$S_n\left[\alpha_{A,n} t_{A,m} + (1-\alpha_{A,n}) t_{B,m}\right] \tag{24}$$

The total volume occupied by all the layers is simply the sum of Eqs. 22 to 24

$$\begin{aligned} V_T = {} & (S_1 + S_2 + \cdots + S_n)\left[\alpha_{A,1} t_{A,m} + (1-\alpha_{A,1}) t_{B,m}\right] \\ & + (S_2 + S_3 + \cdots + S_n)\left[\alpha_{A,2} t_{A,m} + (1-\alpha_{A,2}) t_{B,m}\right] \\ & + \cdots + S_n\left[\alpha_{A,n} t_{A,m} + (1-\alpha_{A,n}) t_{B,m}\right] \end{aligned} \tag{25}$$

Knowing the total volume adsorbed we can calculate the average thickness of the adsorbed layer as $t = V_T/(S_0 + S_1 + S_2 + \cdots S_n)$. Substituting V_T from Eq. 25 and S_i from Eqs. 19, we derive the following equation for the average thickness for the adsorbed layer

$$t = \frac{\left\{\begin{array}{l} (E_1 + E_1E_2 + \cdots + E_1E_2\cdots E_n)\left[\alpha_{A,1} t_{A,m} + (1-\alpha_{A,1}) t_{B,m}\right] \\ + (E_1E_2 + E_1E_2E_3 + \cdots + E_1E_2\cdots E_n)\left[\alpha_{A,2} t_{A,m} + (1-\alpha_{A,2}) t_{B,m}\right] \\ + \cdots + E_1E_2\cdots E_n\left[\alpha_{A,n} t_{A,m} + (1-\alpha_{A,n}) t_{B,m}\right] \end{array}\right\}}{(1 + E_1 + E_1E_2 + \cdots + E_1E_2\cdots E_n)} \tag{26}$$

Having known the average thickness, we can calculate the average remaining width as $H-2t-\sigma_{ss}$, where σ_{ss} is the collision diameter of the carbon atom. Here the pore width H is taken as the distance between the plane passing through the centers of the carbon atoms residing on the outermost layer of one wall to that of the opposite wall.

Adsorbed Concentration. Using the same procedure as was used for the average thickness, we can obtain the average thickness contributed by species A and B, as given below

$$t_A = \frac{\left\{ \begin{array}{l} (E_1 + E_1E_2 + \cdots + E_1E_2\cdots E_n)\alpha_{A,1}t_{A,m} \\ +(E_1E_2 + E_1E_2E_3 + \cdots + E_1E_2\cdots E_n)\alpha_{A,2}t_{A,m} + \cdots + E_1E_2\cdots E_n\alpha_{A,n}t_{A,m} \end{array} \right\}}{(1 + E_1 + E_1E_2 + \cdots + E_1E_2\cdots E_n)} \tag{27a}$$

and

$$t_B = \frac{\left\{ \begin{array}{l} (E_1 + E_1E_2 + \cdots + E_1E_2\cdots E_n)(1-\alpha_{A,1})t_{B,m} \\ +(E_1E_2 + E_1E_2E_3 + \cdots + E_1E_2\cdots E_n)(1-\alpha_{A,2})t_{B,m} + \cdots + E_1E_2\cdots E_n(1-\alpha_{A,n})t_{B,m} \end{array} \right\}}{(1 + E_1 + E_1E_2 + \cdots + E_1E_2\cdots E_n)} \tag{27b}$$

respectively. Knowing the specific volume of the pore as W (m^3/kg), the molar adsorbed concentrations of A and B (mol/kg) are

$$C_{\mu,A} = \frac{W}{v_{A,M}}\left(\frac{2t_A}{H-\sigma_{ss}}\right) \tag{28a}$$

$$C_{\mu,B} = \frac{W}{v_{B,M}}\left(\frac{2t_B}{H-\sigma_{ss}}\right) \tag{28b}$$

and the total adsorbed concentration and the overall mole fraction in the adsorbed phase are

$$C_{\mu,T} = C_{\mu,A} + C_{\mu,B} \tag{28c}$$

$$\langle x_A\rangle = \frac{(t_A/v_{A,M})}{[(t_A/v_{A,M}) + (t_B/v_{B,M})]} \tag{28d}$$

$$\langle x_B\rangle = 1 - \langle x_A\rangle \tag{28e}$$

Pore Pressure. The pressures p_A and p_B involved in the solutions obtained so far for the mole fractions, surface area, and layer thickness are the pressures within the pore. These pressures are different from the corresponding pressures in the bulk gas phase due to the potential energy exerted by the pore walls. We estimate the pore pressures from the bulk phase pressures by using the following equation

$$p_A = p_{b,A}\exp\left(\frac{1}{\Omega}\int_\Omega \frac{\varphi(z)}{RT}\,dz\right) \tag{29}$$

where Ω is the remaining pore space that is not taken up by the adsorbed layer. The term inside the bracket of the exponential is the average potential energy of the pore space that is not occupied by the adsorbed layer.

Pore-filling mechanism

We have established a means to calculate the average thickness, the adsorbed quantity under the mechanism of layering, but this molecular layering process will cease once the remaining pore space is small enough and the pressure has reached a threshold pressure when the filling of the remaining space with liquid mixture occurs. This filling process is governed by the Kelvin equation for mixtures as suggested by Okazaki et al. (1978). This equation, written in the present terminology, is

$$H - 2t - \sigma_{ss} = \frac{2\bar{\gamma}\bar{v}_M}{RT\ln\left[\dfrac{P^0_{\text{mix}}(x_{A,n})}{p_A + p_B}\right]} \tag{30}$$

where $P^0_{\text{mix}}(x_{A,n})$ is the mixture equilibrium pressure at the liquid composition of $x_{A,n}$, where n is the number of the last layer just prior to pore filling. The liquid adsorbate at the core is assumed to have the same composition as that of the last molecular layer. This is reasonable, as in the adsorbed layer the distribution of composition can be sustained, because the interactions with the solid are different for different layers. On the other hand, the liquid in the core, once it is formed due to the pore-filling process, is assumed to be uniform, and its composition must be the same as that of the last adsorbed layer, otherwise there will be a discontinuity in composition at the boundary between the last adsorbed layer and the liquid in the core of the pore.

The mixture equilibrium pressure $P^0_{\text{mix}}(x_{A,n})$ either can be obtained from the vapor–liquid equilibrium data or calculated from the Peng-Robinson equation of state (PR EOS). The parameter $\bar{v}_M$ is the mixture liquid molar volume, and it can be calculated from PR-EOS. The other parameter $\bar{\gamma}$ is the average surface tension, and it can be estimated from

$$\bar{\gamma} = x_{A,n}x_A + (1 - x_{A,n})\gamma_B \tag{31}$$

Mechanism of adsorption in a given pore

We have established the mechanism of adsorption for mixtures in pores (irrespective of the pore size) as one with two processes occurring consecutively:

Stage 1 is the stage where molecular layering occurs, with enhancement allowed for in both the adsorption layer (through the first layer) and in the pore fluid

2. Stage 2 is the stage where pore filling occurs.

What we need to establish next is the condition for the switching over between the two stages in a pore of a given width H. This is described in the following procedure:

1. For a given total pressure in the gas phase and its mole fractions, calculate the average layer thickness, t, from Eq. 26. Knowing this thickness we can determine the average number of layers as $n = t/t_m$, where t_m is the average monolayer thickness.

2. Knowing the number of layers, we calculate the mole fraction of the last layer (nth layer) from Eq. 17b.

3. From the vapor–liquid equilibrium data or from the PR EOS, calculate the mixture equilibrium pressure $P^0_{\text{mix}}(x_{A,n})$ and the liquid molar volume for the mixture. Knowing this we determine the critical pore width as follows

$$H_c = 2t + \sigma_{ss} + \frac{2\bar{\gamma}\bar{v}_M}{\text{RT} \ln\left[\dfrac{P^0_{\text{mix}}(x_{A,n})}{p_A + p_B}\right]} \tag{32}$$

4. If the pore width is greater than this critical pore width, the pore is layered with adsorbed A and B molecules, and the number of layers is n. The adsorbed concentrations for A and B are given in Eqs. 28.

5. However, if the pore width is less than the critical pore width ($H < H_c$), then the pore is completely filled with adsorbates contributed by molecules from species A and B. The task here is to determine the total pressure at which the onset of pore filling occurs. Let p^*_A and p^*_B be the pressures when the pore is just about to be filled. At these pressures, the layer thickness as calculated from Eq. 26 is denoted as t^*. We shall determine the total pressure $P^* = p^*_A + p^*_B$ at the instant of pore filling as follows. Let the mole fraction of A at the top of adsorbed layer be x^*_A. The total pressure P^* is then calculated from the Kelvin equation for mixtures evaluated at the composition x^*_A and the thickness t^*

$$H = 2t^* + \sigma_{ss} + \frac{2\bar{\gamma}\bar{v}_M(x^*_A)}{RT \ln\left[\dfrac{P^0_{\text{mix}}(x^*_A)}{P^*}\right]} \tag{33}$$

Here P^* is solved from this equation in conjunction with Eq. 26. In Eq. 33, $P^0_{\text{mix}}(x^*_A)$ is the mixture equilibrium pressure at the composition x^*_A, and $\bar{\gamma}$ is the average surface tension evaluated at the same composition. Knowing the thickness of the layer t^*, the average thickness contributed by species A and B are t^*_A and t^*_B. If the volume of that pore is W, the adsorbed concentrations of A and B contributed by the adsorbed layer are

$$C_{\mu,A} = \frac{W}{v_{A,M}}\left(\frac{2t^*_A}{H - \sigma_{ss}}\right) \tag{34a}$$

$$C_{\mu,B} = \frac{W}{v_{B,M}}\left(\frac{2t^*_B}{H - \sigma_{ss}}\right) \tag{34b}$$

The remaining core is filled with a liquid mixture with a composition x^*_A. Thus, the total concentrations of A and B are

$$C_{\mu,A} = \frac{W}{v_{A,M}}\left(\frac{2t^*_A}{H - \sigma_{ss}}\right) + \frac{W}{v_{A,M}}\left(\frac{H - \sigma_{ss} - t^*}{H - \sigma_{ss}}\right)x^*_A \tag{35a}$$

$$C_{\mu,B} = \frac{W}{v_{B,M}}\left(\frac{2t^*_B}{H - \sigma_{ss}}\right) + \frac{W}{v_{B,M}}\left(\frac{H - \sigma_{ss} - t^*}{H - \sigma_{ss}}\right)(1 - x^*_A) \tag{35b}$$

Equations 35 describe the local adsorption isotherm for a pore of width H. For a solid with a pore-size distribution, the overall adsorption isotherm is the sum of isotherms of all pores weighted with respect to the pore volume distribution. This is done in the next subsection.

Adsorption isotherm

The theory presented in this article provides us with a means of calculating the adsorption isotherm when the pore-size distribution and the BET constant for a corresponding flat surface are known for all adsorbates. We let $f(H)$ be the pore volume distribution (m^3/kg/m), with $f(H)\,dH$ being the volume of pores having a width that falls between H and $H + dH$. The total pore volume (including all pores, m^3/kg) is calculated from

$$W_0 = \int_{\sigma_{ss}}^{\infty} f(H)\,dH \tag{36}$$

Thus, for the given bulk gas phase pressures $p_{b,A}$ and $p_{b,B}$, the critical pore width calculated from Eq. 32 is denoted as $H_c(p_{b,A}, p_{b,B})$, and pores having size smaller than this critical width will be filled with adsorbates of species A and B while for pores with a size greater than H_c layering of molecules is occurring. Mathematically, the overall adsorbed concentration (in mole/kg) for A and B are given by

$$C_{\mu,A} = \frac{1}{v_{A,M}}\int_{\sigma_{ss}}^{H_c(p_{b,A},\,p_{b,B})}\left[\left(\frac{2t^*_A(H)}{H - \sigma_{ss}}\right) + \left(\frac{H - \sigma_{ss} - t^*(H)}{H - \sigma_{ss}}\right)x^*_A(H)\right]f(H)\,dH + \frac{1}{v_{A,M}}\int_{H_c(p_{b,A},p_{b,B})}^{\infty}\left(\frac{2t_A(H)}{H - \sigma_{ss}}\right)f(H)dH \tag{37a}$$

$$C_{\mu,B} = \frac{1}{v_{B,M}}\int_{\sigma_{ss}}^{H_c(p_{b,A},p_{b,B})}\left[\left(\frac{2t^*_B(H)}{H - \sigma_{ss}}\right) + \left(\frac{H - \sigma_{ss} - t^*(H)}{H - \sigma_{ss}}\right)(1 - x^*_A(H))\right]f(H)\,dH + \frac{1}{v_{B,M}}\int_{H_c(p_{b,A},p_{b,B})}^{\infty}\left(\frac{2t_B(H)}{H - \sigma_{ss}}\right)f(H)\,dH \tag{37b}$$

Equations 37 provide the mathematical representation of the overall adsorption isotherm, that is, given a distribution $f(H)$, one can simply integrate Eq. 37 to obtain the overall adsorbed concentration. In the literature, many workers have assigned a continuous distribution function (or a combination of continuous functions) to describe the pore-size distribution, with continuous distribution functions such as normal, log-normal, gamma, beta distribution functions. However, micropore size distribution is expected to be very irregular, and it is difficult to properly describe it with a continuous function or even a combination of continuous functions. What we shall do here is to present a discrete way of presenting the pore-size distribution, that is, the PSD is mathematically described by a set of

$$(H_i, W_i) \qquad \text{for} \quad i = 1, 2, \ldots, m \tag{38}$$

where the pore range has been divided into m subranges, and for the ith subrange the representative pore width is H_i and the total pore volume of that subrange is W_i. Let H_M be the pore width of the Mth subrange such that all subranges having $H_i < H_M$ will be filled with adsorbate molecules, while the other subranges having widths greater than H_M will be layered with adsorbate molecules. With this discrete formulation, the adsorbed concentrations of Eqs. 37 would be replaced by

$$C_{\mu,A} = \frac{1}{v_{A,M}} \sum_{j=1}^{M} \left[\left(\frac{2t_A^*(H_j)}{H_j - \sigma_{ss}} \right) + \left(\frac{H_j - \sigma_{ss} - t^*(H_j)}{H_j - \sigma_{ss}} \right) x_A^*(H_j) \right] W_j + \frac{1}{v_{A,M}} \sum_{j=M+1}^{n} \left(\frac{2t_A(H_j)}{H_j - \sigma_{ss}} \right) W_j \tag{39a}$$

$$C_{\mu,B} = \frac{1}{v_{B,M}} \sum_{j=1}^{M} \left[\left(\frac{2t_B^*(H_j)}{H_j - \sigma_{ss}} \right) + \left(\frac{H_j - \sigma_{ss} - t^*(H_j)}{H_j - \sigma_{ss}} \right) \left(1 - x_A^*(H_j)\right) \right] W_j + \frac{1}{v_{B,M}} \sum_{j=M+1}^{n} \left(\frac{2t_B(H_j)}{H_j - \sigma_{ss}} \right) W_j \tag{39b}$$

For computation, the following algorithm can be used:

(1) Start with $i = 1$;

(2) For given pressures $p_{b,A}$ and $p_{b,B}$, calculate the pore pressure from Eq. 29;

(3) Check to see whether the pore is either filled or layered by investigating the following inequality

$$H > 2t + \sigma_{ss} + \frac{2\bar{\gamma}\bar{v}_M}{\mathrm{RT} \ln \left[\dfrac{P^0_{\mathrm{mix}}(x_{A,n})}{p_A + p_B} \right]}$$

If this is true, then pores are layered with adsorbate molecules of A and B having the following respective concentrations

$$\frac{1}{v_{A,M}} \left(\frac{2t_A(H_i)}{H_i - \sigma_{ss}} \right) W_i \qquad \text{and} \qquad \frac{1}{v_{B,M}} \left(\frac{2t_B(H_i)}{H_i - \sigma_{ss}} \right) W_i$$

otherwise, the pore will be filled with the following adsorbate concentrations

$$C_{\mu,A} = \frac{1}{v_{A,M}} \left[\left(\frac{2t_A^*(H_i)}{H_i - \sigma_{ss}} \right) + \left(\frac{H_i - \sigma_{ss} - t^*(H_i)}{H_i - \sigma_{ss}} \right) x_A^*(H_i) \right] W_i$$

$$C_{\mu,B} = \frac{1}{v_{B,M}} \left[\left(\frac{2t_B^*(H_i)}{H_i - \sigma_{ss}} \right) + \left(\frac{H_i - \sigma_{ss} - t^*(H_i)}{H_i - \sigma_{ss}} \right) \left(1 - x_A^*(H_i)\right) \right] W_i$$

(4) Repeat the steps 1 to 3 until all subranges have been dealt with

(5) The total adsorbed concentration is the sum of the adsorbed concentrations of all subranges.

Simulations

Before validating our theory by comparing it with the experimental data, we carry out simulations to study the effects of BET constant for a flat surface, surface tension, total pressure, and temperature on the adsorption equilibria of the binary systems. The information required for the computation are:

(1) The pore-size distribution
(2) The BET constant for a flat surface
(3) The vapor–liquid equilibrium information
(4) The surface tension.

The pore-size distribution used in our simulation is obtained from the analysis of data of benzene adsorption on a commercial activated carbon from a very low reduced pressure of 10^{-5} up to that very close to the vapor pressure. These data are available in our laboratory, and are shown in Figure 2 for the benzene isotherm at 303 K. Using the pore-size

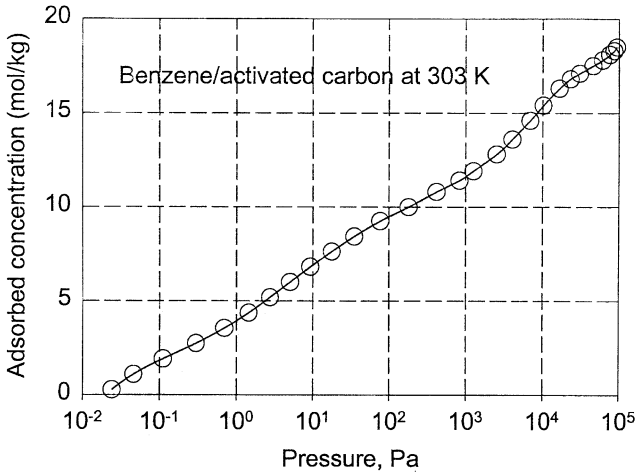

Figure 2. Isotherm of benzene/AC at 303 K.

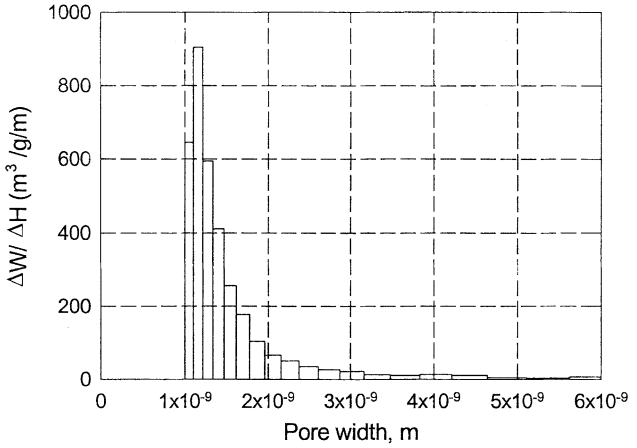

Figure 3. Pore-size distribution of activated carbon.

distribution analysis developed by Do et al. (2001), the pore-size distribution presented as a histogram is shown in Figure 3. This activated carbon is typical of many other commercially activated carbons. It has the following properties: total pore volume of 0.67 cm^3/g, BET surface area of 1200 m^2/g, and micropore volume of 0.48 cm^3/g.

The BET constants for pure substances on nonporous carbon black are available in various publications in the literature. Some of these values are listed in Table 2.

The vapor–liquid equilibrium is readily available in the literature, or alternatively, it can be effectively computed from the Peng–Robinson equation of state (Sandler, 1999). Finally, the surface-tension information is also available in the literature (Jasper, 1972).

We will take a binary system of A and B, with A being the more volatile species. The vapor–liquid equilibrium of this mixture is shown in Figure 4a as plots of the bubble pressure and dew-point pressure vs. mole fraction of A, and in Figure 4b as plots of f_A and f_B vs. x_A (see Appendix B).

The base parameters for the BET constants for A and B on a flat surface are 15 and 35, and those for surface tension are 0.004 and 0.007 Nm^{-1}, respectively. The BET constants means that on a nonporous surface B is a stronger adsorbing species.

Effect of BET constant

Figure 5 shows the effects of the BET constant of A on the x-y selectivity diagram. When the BET constant of A is less than that of B (curve A), the adsorption system is favorable toward B as expected, because B is a lesser volatile species and adsorbs stronger on a surface. When the BET constant of A is increased from 15 to 50, making species A a stronger adsorbing species on a surface, the selectivity of the system is still favorable toward B (curve B) due to the vapor–liquid equilibrium, where B is a less volatile species, which is a dominating factor. The same is still true when BET constant is increased to 100 (curve C). However, when that constant is increased to 300, the system selectivity is reversed, and A is the more favorable species. This is due to the much stronger adsorbing characteristics of A toward a surface that is now significant enough to overcome its greater volatility in the vapor–liquid equilibrium. This interesting behavior is one of the reasons for various patterns of selectivity in the adsorption of mixtures.

Table 2. BET Constants for Various Species on Nonporous Carbon Black

Species	T (K)	BET constant	References
Benzene	293	70.1	Isirikyana and Kieselev (1961)
Toluene	261.7	186.7	Pierce and Ewing (1967)
	273	163.6	
	298	126.5	
n-Pentane	293	40.2	Beebe et al. (1947, 1950)
n-Hexane	293	310	Isirikyan and Kiselev (1961)
Ethane	212.7	21.4	Avgul et al. (1973)
	293	14.1	
Ethylene	212.7	30.7	Avgul et al. (1973)
Propylene	293	38.6	Beebe et al. (1947)
Cyclohexane	245	91	Pierce and Ewing (1967)
	298	52.6	

Effect of surface tension

The effect of surface tension is illustrated in Figure 6, where we see that it has only a very small effect on the selectivity. Note that we have made a large change, from 0.004 to 0.03, in surface tension of species A. What this suggests is

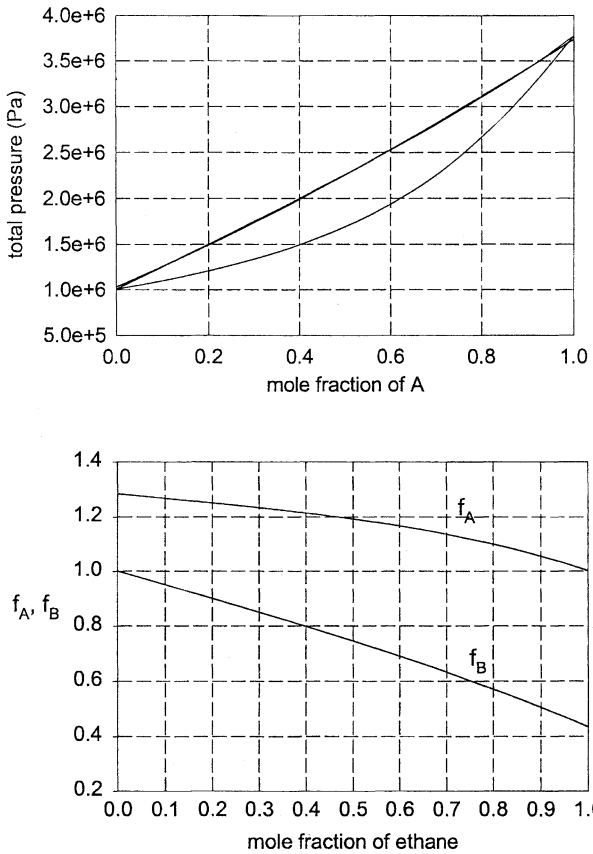

Figure 4. (a) Vapor–liquid equilibrium curve, and (b) the functional forms for f_A and f_B (Eqs. B4 and B5).

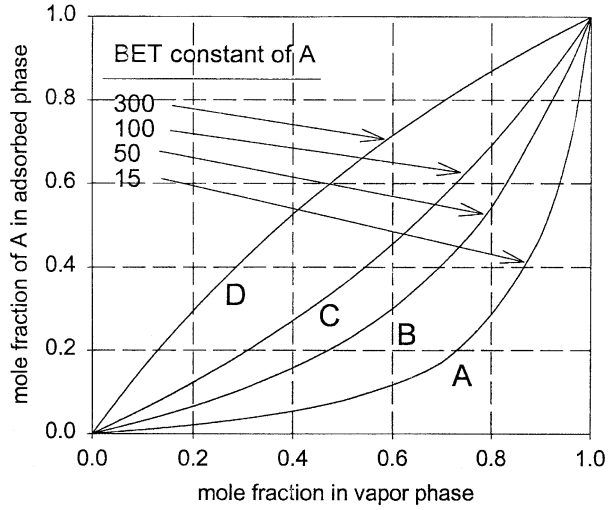

Figure 5. Effect of BET constant.

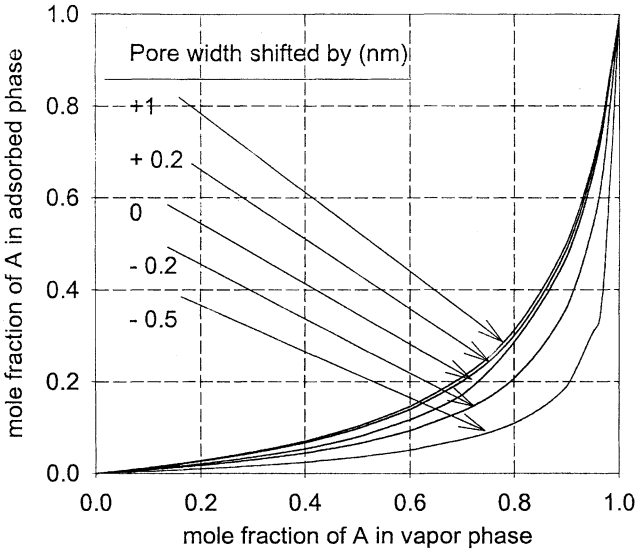

Figure 7. Effect of pore-size distribution on the selectivity behavior.

that the accurate determination of surface tension is not critical in the adsorption of mixtures in a porous media.

Effect of PSD

The effect of the pore-size distribution on the selectivity is shown in Figure 7, where the curves are simulated using the PSD as shown in Figure 3, with the shift either to the right (toward large micropores) or to the left (toward small micropores). We see that the shift of pores toward smaller micropores has a greater effect than that toward large micropores. Nevertheless, the shift has to be significant to have a significant influence on the selectivity. What this implies is that if most commercial activated carbons are well developed, they tend to have a comparable micropore distribution, with the mean pore width about 1 nm or so. Figure 7 suggests that as long as all activated carbons have a mean width of 1 ± 0.2 nm, the effect of PSD on the selectivity is modest. Although the PSD does not significantly affect much the selectivity, it does affect the absolute capacities of species A and B. For example, at 10 kPa, 293 K, and 50:50 mixture in the gas phase, the adsorptive capacities for A and B are 0.15 and 1.77 mol/kg, respectively. If the PSD is shifted to the right by 0.2 nm (toward larger micropores), the capacities are expected to be lower due to the lower adsorption affinities in larger pores. Indeed, this is the case; the adsorptive capacities when PSD is shifted by 0.2 nm are 0.076 and 0.7 mol/kg. Likewise if we shift the PSD to the left (that is, to smaller pore size) by 0.2 nm, the capacities are 0.22 and 3.2 mol/kg, which are indeed greater due to the higher adsorption affinity of smaller pores.

Effect of total pressure

The effects of total pressure on the selectivity are shown in Figure 8, where the total pressure has values of 1, 10, and 50 kPa. We see that the total pressure has a modest effect on

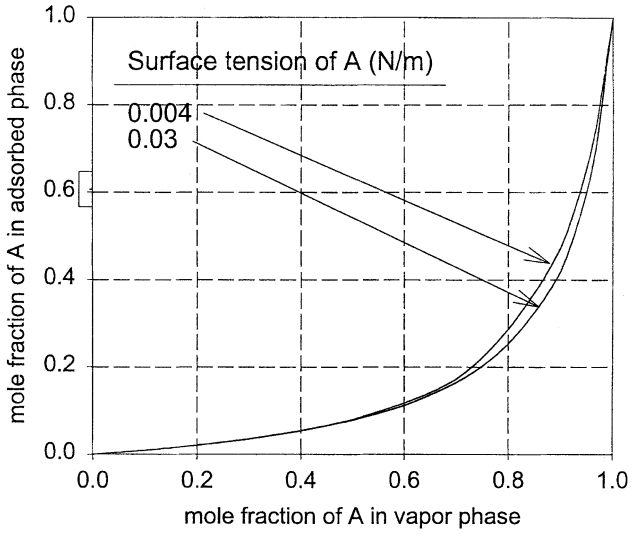

Figure 6. Effect of surface tension on the selectivity diagram.

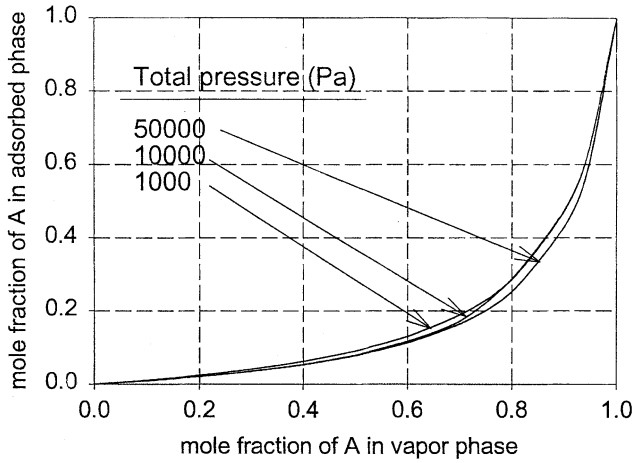

Figure 8. Effect of total pressure on the selectivity behavior.

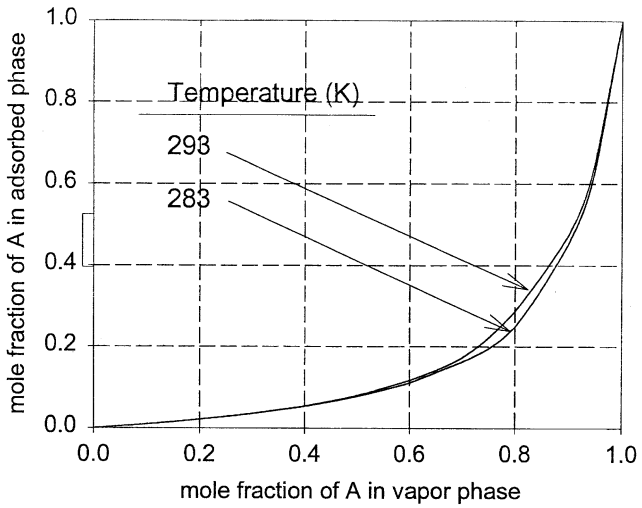

Figure 9. Effect of temperature on the selectivity behavior.

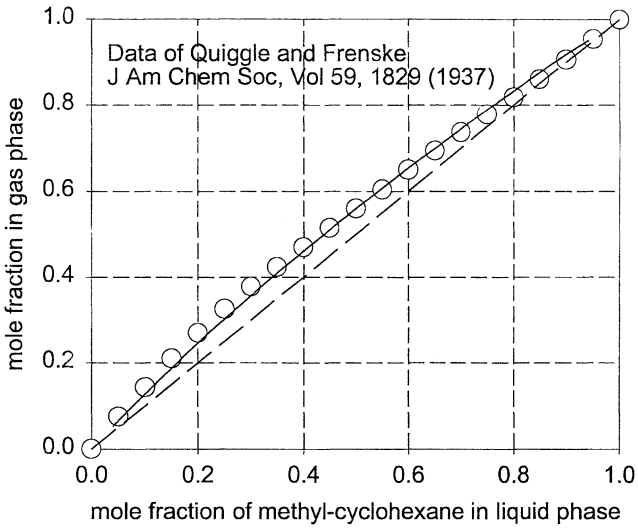

Figure 10. Vapor–liquid equilibrium data of methyl-cyclohexane/toluene.

the selectivity. Although the total pressure does not affect the selectivity, it does affect the capacities. The higher the pressure, the greater the adsorption capacities, as one would expect physically. For example, for a 50:50 gaseous mixture at a total pressure of 1 kPa, the adsorption capacities of A and B are 0.017 and 0.184 mol/kg, respectively. While at a higher pressure of 10 kPa, the corresponding adsorption capacities are 0.27 and 3.22 mol/kg, respectively.

Effect of temperature

Last, we finally study the effect of temperature. This is shown in Figure 9 where we present plots of the selectivity vs. the mole fraction of A in the vapor phase with the temperature as the parameter (283 and 293 K). Once again, the selectivity does not vary with the temperature, but it does affect the adsorption capacities. The higher the temperature is, the lower the adsorption capacity. For example, at 10 kPa and 283 K, the adsorptive capacities of A and B are 0.27 and 3.22 mol/kg, respectively, while their capacities are 0.15 and 1.77 mol/kg at the same total pressure but at a higher temperature of 293 K.

Comparison with Experimental Data

We illustrate the theory presented in this article with experimental data that are available in the literature. The various binary systems considered in this article are:

1. Methyl-cyclohexane/toluene/activated carbon at 298 K (Yu and Neretnieks, 1990)

(2) Ethane/propylene/activated carbon at 293 K (Costa et al., 1981)

(3) Ethylene/ethane/activated carbon at 212.7 K (Reich et al., 1980)

(4) Benzene/*n*-hexane/activated carbon at 293 K (Xie et al., 1998)

(5) Benzene/*n*-pentane/activated carbon at 293 K (Xie et al., 1998)

(6) *n*-hexane/*n*-pentane/activated carbon at 293 K (Xie et al., 1998).

Methyl cyclohexane/toluene/AC (Yu and Neretnieks' data)

To use the Peng–Robinson equation to generate the vapor–liquid equilibrium data, we require a value for the binary interaction parameter used in the mixing rule (Eqs. C3c). Since this parameter is not available in the literature, we matched the calculations from the Peng–Robinson equation with the experimental data of the vapor–liquid equilibrium of Quiggle and Frenske (1937). We found that the optimal value for the binary interaction parameter k_{ij} is zero, and the agreement between the theory and the data is shown in Figure 10.

Having the interaction parameter, we calculate the vapor–liquid equilibrium for methyl-cyclohexane/toluene at 298 K, and the results are plotted in Figures 11 as f_A and f_B vs. the mole fraction of methyl-cyclohexane in the liquid phase, and the equilibrium bubble and dew-point pressures vs. the mole fraction of methyl-cyclohexane in the liquid phase. We found that methyl-cyclohexane is the more volatile species.

The functional form for f_A and f_B and the equilibrium pressure for mixture are fitted with a polynomial, and these polynomials are then used in the theory to calculate the adsorption equilibria. The prediction for the adsorption equilibria against the experimental results of Yu et al. is shown in Figure 12 as a plot of the mole fraction in the adsorbed phase vs. the mole fraction in the vapor phase. The surface tensions for methyl-cyclohexane and toluene are 0.02329 and 0.02793 Nm^{-1} (Jasper, 1972). Their corresponding BET constants for a flat surface are 52 and 126. We see that for this system methyl-cyclohexane is the weaker adsorbing species as well as a more volatile species. Therefore, we expect the adsorption system is more favorable toward toluene, as seen in Figure 12.

The agreement seems reasonable, but there is a small deviation when the mole fraction of methyl-cyclohexane is high in the vapor phase. The source of this deviation is not easy to identify, but there are a number of possible reasons for this deviation. For example, the model is inadequate, the choice of pore-size distribution used in our model may not exactly

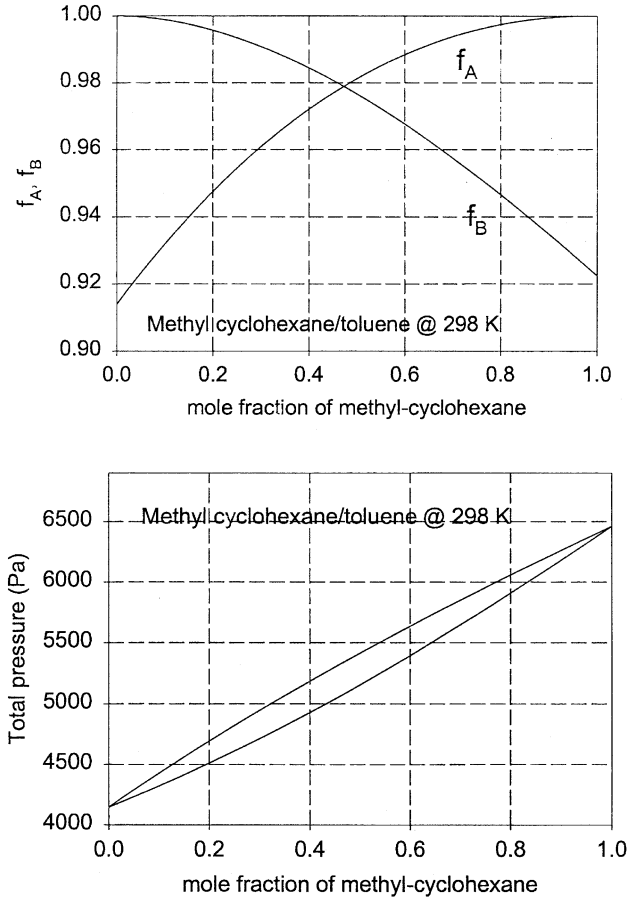

Figure 11. (a) Plots of f_A and f_B, and (b) total equilibrium pressure vs. the mole fraction of methyl-cyclohexane in the condensed phase.

describe the PSD of the activated carbon used by Yu and Neretnieks, and the possible errors associated with the experiments. We need to have more accurate data for mixtures in the literature before we can draw firm conclusions about the feasibility of a model as a predicting tool.

Ethane/propylene/AC (data of Costa et al., at 293 K)

In this section, we consider the data of Costa et al. for adsorption of ethane and propylene on activated carbon. The solid used by Costa et al. has the following properties: BET surface area of 700 m^2/g, total porosity of 0.715, particle density of 0.795 g/cm^3, and solid density of 2.7 g/cm^3. For this combination of ethane and propylene, the binary interaction parameter is 0.089 (Sandler, 1999). With this parameter, the PR EOS is used to generate vapor–liquid equilibrium pressure and the functions f_A and f_B as function of the mole fraction of ethane. From this vapor–liquid equilibrium study, ethane is the more volatile species.

The BET constants for ethane and propylene are 14 and 38.6, respectively (Table 2). The surface tensions are taken from Jasper, and their respective values are 0.004 and 0.007 Nm^{-1}. Since propylene is the less volatile species and its BET constant for a flat surface is greater, we expect that the solid will have a strong preference toward propylene. Indeed this

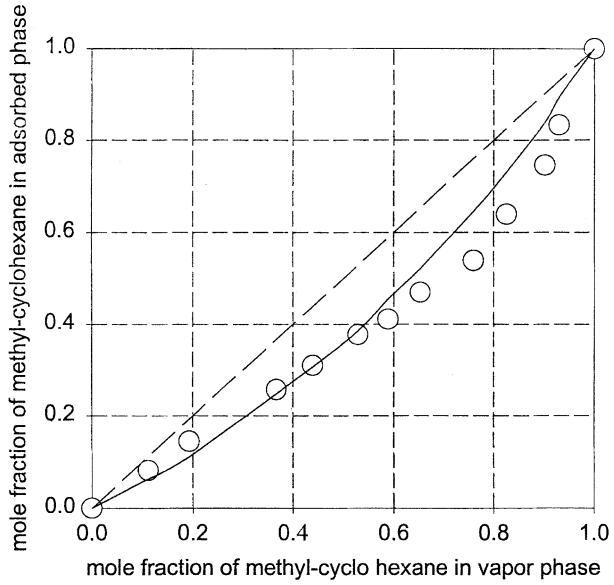

Figure 12. $x = y$ Selectivity diagram for the system of methyl-cyclohexane (Yu and Neretrieks, 1990).

is the case, as seen in Figure 13 where we plot the mole fraction of ethane in the adsorbed phase vs. its mole fraction in the vapor phase. Here the total pressure is 10 kPa. The continuous line is the prediction from this model, while the symbols are experimental data of Costa et al. (1981) at 293 K. We see that the prediction by the theory is regarded as very good.

Ethylene/ethane/AC (data of Reich et al.)

Next we test the model with the data of adsorption of ethylene and ethane at 212.7 K collected by Reich et al. (1980). The binary interaction parameter of 0.01 (Sandler, 1999) is used in the Peng–Robinson equation to generate information

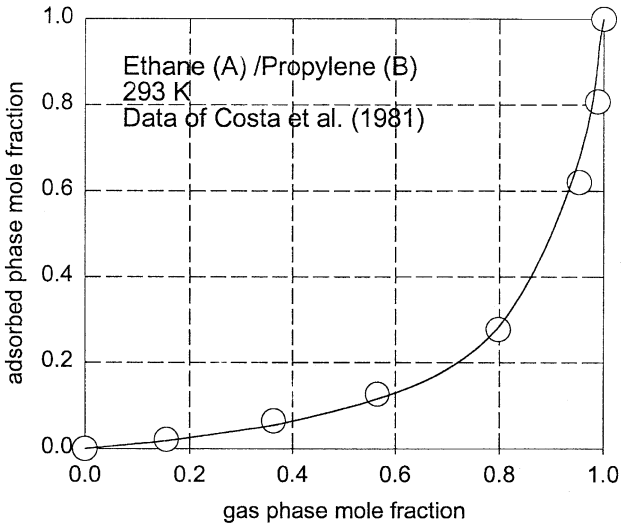

Figure 13. x-y Selectivity diagram for the system of ethane/propylene (Costa et al., 1981).

Table 3. The Predictions of Ethylene/Ethane/Activated Carbon System at 212.7 K

Pressure (Pa)	Mol Fract. of Ethylene in Vapor Phase	Adsorbed Phase Mole Fractions	Calc. Ads. Phase Mol Fraction	% Error
405,200	0.76	0.675	0.652	3.4
223,960	0.76	0.667	0.671	0.6
139,890	0.76	0.654	0.671	0.26
343,180	0.318	0.226	0.201	11
240,500	0.318	0.221	0.201	9.0
137,134	0.318	0.210	0.224	6.7

on the vapor–liquid equilibrium, and the functions f_A and f_B as a function of the mole fraction of ethylene. From the vapor–liquid equilibrium, we find that ethylene is the more volatile species. The BET constants for a flat surface for ethylene and ethane are 30.7 and 21.4, respectively (Table 2). Even though ethylene has a higher BET constant (that is, it is preferential to a flat surface over ethane), its higher volatility has made it less attractive to the pores of activated carbon. This is illustrated in Table 3, where we see that activated carbon is preferred by ethane. The agreement between the theory and the experimental data is reasonable. The maximum percentage error observed from the table is about 10%. Like the case of methyl-cyclohexane/toluene, the deviation could be for a number of reasons, and it is difficult to point to the actual source of deviation.

Data of Xie et al.

Now we consider the experimental data of Xie et al. (1998) with three sets of binary systems: (1) benzene/*n*-hexane/activated carbon, (2) benzene/*n*-pentane/activated carbon, and (3) *n*-hexane/*n*-pentane/activated carbon. The adsorption temperature is 293 K for all these systems.

Benzene/n-Hexane/Activated Carbon. Similar to the previous systems studied, the vapor–liquid equilibrium for benzene and *n*-hexane is obtained from the PR-EOS, from which we find that benzene is the less volatile species.

From the adsorption on a nonporous surface, *n*-hexane is a stronger adsorbing species (C_{BET} of 422 for *n*-hexane compared to 70 for benzene), but the vapor–liquid equilibrium strongly favors benzene in the condensed phase, resulting in a better selectivity of benzene in adsorption in porous media, as shown in Table 4.

A large percentage error is observed for one particular run where the benzene mole fraction is very low ($y = 0.043$). This is attributed to possible experimental errors because of

Table 4. Benzene (1)/*n*-Hexane (2) Binary Data

Pres. (Pa)	Mol Fract. of Benzene in Vapor Phase	Mol Fract. of Benzene in Ads. Phase	Calc. Mol Fract. of Benzene	% Error
770	0.912	0.926	0.928	0.2
803	0.823	0.839	0.863	2.8
981	0.674	0.682	0.757	11.0
1,130	0.460	0.506	0.572	13
1,100	0.278	0.355	0.370	4.2
1,260	0.107	0.191	0.150	21
1,530	0.043	0.102	0.06	41

Table 5. Benzene (1)/*n*-Pentane (2) Binary Data

Pres. (Pa)	Mol Fract. of Benzene in Vapor Phase	Mol Fract. of Benzene in Ads. Phase	Calc. Mol Fraction of Benzene	% Error
1,060	0.723	0.925	0.940	1.6
967	0.623	0.907	0.913	0.7
1,080	0.369	0.741	0.789	6.5
1,220	0.207	0.571	0.626	9.6
1,420	0.100	0.425	0.417	1.9
1,420	0.044	0.218	0.229	5.0
1,580	0.016	0.116	0.0951	18.0

a much better agreement between the theory and the data for all other runs.

Benzene/n-Pentane/Activated Carbon. The vapor–liquid equilibrium for benzene and *n*-pentane is generated from the PR-EOS, from which we find that benzene is the less volatile species. Since benzene has a higher BET constant for a flat surface than does *n*-pentane, we expect a favorable selectivity of benzene toward the carbon media. This is indeed seen in Table 5 and Figure 14. Here we see that the agreement is regarded as excellent.

n-Hexane/n-Pentane/Activated Carbon. Lastly, we test the model with the adsorption data of *n*-hexane and *n*-pentane on activated carbon. The vapor–liquid equilibrium is obtained, from which we find that *n*-hexane is the less volatile species. Since *n*-hexane is a stronger adsorbing species (larger C-BET constant) than *n*-pentane and is less volatile, we would expect *n*-hexane to be the dominant in the adsorbed phase of a porous media. This can indeed be seen in Table 6 and Figure 15. As in the previous systems, agreement between the theoretical prediction and the data is very good.

We have applied the theory for adsorption of mixtures containing subcritical adsorbates to a number of systems whose experimental data are available in the literature. Although the agreement is reasonable for all systems tested, the applicability of the theory is limited to systems with ad-

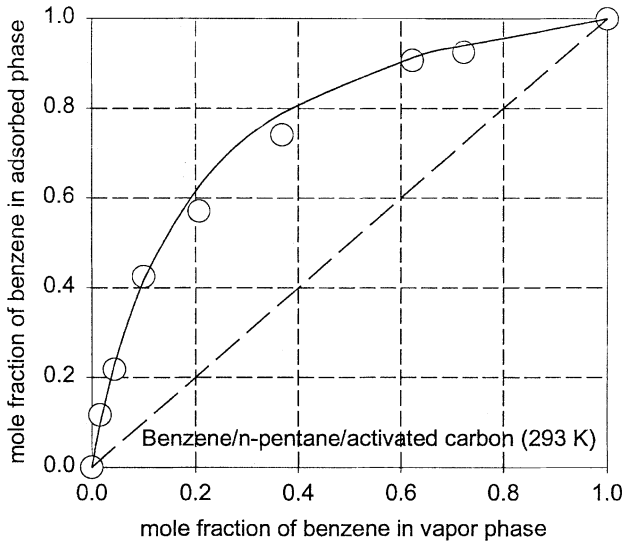

Figure 14. *x-y* Selectivity diagram for the system of benzene/*n*-pentane (Xie et al., 1998).

Table 6. *n*-Hexane (1)/*n*-Pentane (2) Binary Data

Pres. (Pa)	Mol Fract. of Benzene in Vapor Phase	Mol Fract. of Benzene in Ads. Phase	Calc. Mol Fraction of Benzene	% Error
670	0.693	0.949	0.936	1.4
523	0.509	0.896	0.887	1.0
599	0.284	0.722	0.765	6.0
846	0.140	0.570	0.573	0.5
663	0.073	0.377	0.396	5.0
696	0.024	0.186	0.172	7.5
648	0.009	0.091	0.0715	21.0

sorbates of similar behavior because of the number of the model's inherent limitations. The model should not be applicable to systems

1. Containing mixtures of subcritical adsorbates and supercritical adsorbates
2. Containing polar compounds.

Conclusions

In this article we have given a theory for predicting adsorption equilibria of the binary systems of subcritical fluids. The information required for the prediction are the pore size distribution, the BET constant of the pure component for a corresponding flat surface, such as the carbon black, and information on the vapor–liquid equilibrium, which can be obtained from the PR EOS. The process of adsorption occurs in two consecutive stages: layering and pore filling. Comparison of the theory with a large number of experimental data shows that the theory is a valuable tool in the prediction of adsorption equilibria for mixtures of subcritical fluids.

Acknowledgment

This work is supported by the Australian Research Council.

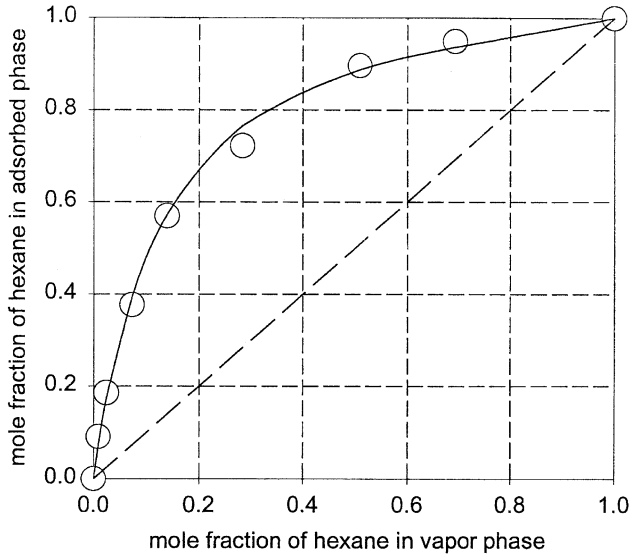

Figure 15. *x*-*y* Selectivity diagram for the system of *n*-hexane/*n*-pentane (Xie et al., 1998).

Literature Cited

Avgul, N. N., A. G. Bezus, E. S. Dobova, and A. V. Kiselev, "The Similarity of Gas Adsorption by Non-Porous and Microporous Crystalline Adsorbents," *J. Colloid Interface Sci.*, **42**, 486 (1973).

Beebe, R., M. Polley, W. Smith, and C. Wendell, "Heats of Adsorption on Carbon Black. II," *J. Amer. Chem. Soc.*, **69**, 2294 (1947).

Beebe, R., G. Kington, M. Polley, and W. Smith, "Heats of Adsorption and Molecular Configuration. The Pentanes on Carbon Black," *J. Amer. Chem. Soc.*, **72**, 40 (1950).

Cook, W., and D. Basmadjian, "The Prediction of Binary Adsorption Equilibria from Pure Component Isotherms," *Can. J. Chem. Eng.*, **30**, 78 (1965).

Costa, E., J. L. Sotelo, G. Calleja, and C. Marron, "Adsorption of Binary and Ternary Hydrocarbon Gas Mixtures on Activated Carbon: Experimental Determination and Theoretical Prediction of the Ternary Equilibrium Data," *AIChE J.*, **27**, 5 (1981).

Do, D. D., *Adsorption Analysis: Equilibria and Kinetics*, Imperial College Press, London (1998a).

Do, D. D., "Pore Size Distribution of Micro and Mesoporous Materials by Using a Classical Isotherm Method," Intl. Symp. New Trends in Colloid and Interface Sciences, Chiba, Japan (1998b).

Do, D. D., C. Nguyen, and H. D. Do, "Characterisation of Micro-Mesoporous Carbon Media," *Colloids Surf.*, **187**, 51 (2001).

Do, D. D., and H. D. Do, "Characterization of Micro-Mesoporous Carbonaceous Materials: Calculations of Adsorption Isotherms of Hydrocarbons," *Langmuir*, **18**, 93 (2002).

Dunne, J., and A. Myers, "Adsorption of Gas Mixtures in Micropores: Effect of Difference in Size of Adsorbate Molecules," *Chem. Eng. Sci.*, **49**, 2941 (1994).

Frances, E., F. Siddiqui, D. Ahn, C. H. Chang, and N. H. Wang, "Thermodynamically Consistent Equilibrium Adsorption Isotherms for Mixtures of Different Size Molecules," *Langmuir*, **11**, 3177 (1995).

Frey, D., and A. E. Rodrigues, "Explicit Calculation of Multicomponent Equilibria for Ideal Adsorbed Solutions," *AIChE J.*, **40**, 182 (1994).

Grant, R. J., and M. Manes, "Adsorption of Binary Hydrocarbon Gas Mixtures on Activated Carbon," *Ind. Eng. Chem. Fundam.*, **5**, 490 (1966).

Hill, T., "Theory of Multimolecular Adsorption from a Mixture of Gases," *J. Chem. Phys.*, **14**, 268 (1946).

Hoory, S., and J. Prausnitz, "Monolayer Adsorption of Gas Mixtures on Homogeneous and Heterogeneous Solids," *Chem. Eng. Sci.*, **22**, 1025 (1967).

Isirikyan, A., and A. V. Kiselev, "The Absolute Adsorption Isotherms of Vapors of Nitrogen, Benzene, and n-Hexane and the Heats of Adsorption of Benzene and n-Hexane on Graphitised Carbon Blacks. I. Graphitised Carbon Black," *J. Phys. Chem.*, **65**, 601 (1961).

Jasper, J., "Surface Tension of Liquids," *J. Phys. Chem. Ref. Data*, **1**, 841 (1972).

Karavias, F., and A. Myers, "Molecular Thermodynamics of Adsorption from Gas Mixtures: Composition of Adsorbed Phase from Gravimetric Data," *Chem. Eng. Sci.*, **47**, 1441 (1992).

Koopal, L. K., W. H. van Riemsdijk, J. de Wit, and M. Benedetti, "Analytical Isotherm Equations for Multicomponent Adsorption to Heterogeneous Surfaces," *J. Colloid Interface Sci.*, **166**, 51 (1994).

LeVan, M. D., and T. Vermeulen, "Binary Langmuir and Freundlich Isotherms for Ideal Adsorbed Solutions," *J. Phys. Chem.*, **85**, 3247 (1981).

Lewis, W., E. Gilliland, B. Chertow, and W. Cadogan, "Adsorption Equilibria–Hydrocarbon Gas Mixtures," *Ind. Eng. Chem.*, **42**, 1319 (1950).

Liedy, W., and E. Schlunder, "A New Statistical Model for Adsorption of Mixtures on Heterogeneous Surfaces," *Ber. Bunsenges. Phys. Chem.*, **92**, 4 (1988).

Mehta, S., and R. Danner, "An Improved Potential Theory Method for Predicting Gas Mixture Adsorption Equilibria," *Ind. Eng. Chem. Fundam.*, **24**, 325 (1985).

Moon, H., and C. Tien, "Further Work on Multicomponent Adsorption Equilibria Calculations Based on the Ideal Adsorbed Solution Theory," *Ind. Eng. Chem. Res.*, **26**, 2042 (1987).

Moon, H., and C. Tien, "Adsorption of Gas Mixtures on Adsorbents With Heterogeneous Surfaces," *Chem. Eng. Sci.*, **43**, 2967 (1988).

Myers, A., "Gravimetric Measurement of Adsorption from Binary Gas Mixtures," *Pure and Appl. Chem.*, **61**, 1949 (1989).
Myers, A., and J. M. Prausnitz, "Thermodynamics of Mixed Gas Adsorption," *AIChE J.*, **11**, 121 (1965).
Myers, A., and S. Sircar, "A Thermodynamic Consistency Test for Adsorption of Liquids and Vapors on Solids," *J. Phys. Chem.*, **76**, 3412 (1972).
Myers, A., and D. Valenzuela, "Computer Algorithm and Graphical Method for Calculating Adsorption Equilibria of Gas Mixtures," *J. Chem. Eng. Jpn.*, **19**, 392 (1986).
Nguyen, C., and D. D. Do, "A New Method for the Characterisation of Porous Materials," *Langmuir*, **15**, 3608 (1999).
Nguyen, C., and D. D. Do, "Multicomponent Supercritical Adsorption in Microporous Activated Carbon Materials," *Langmuir*, **17**, 1552 (2001).
O'Brien, J., and A. Myers, "Rapid Calculations of Multicomponent Adsorption Equilibria from Pure Isotherm Data," *Ind. Eng. Chem. Process Des. Dev.*, **24**, 1188 (1985).
O'Brien, J., and A. Myers, "A Comprehensive Technique for Equilibrium Calculations in Adsorbed Mixtures: The Generalized Fast-IAS Method," *Ind. Eng. Chem. Res.*, **27**, 2085 (1988).
Okazaki, M., H. Tamon, and R. Toei, "Prediction of Binary Adsorption Equilibria of Solvent and Water Vapor on Activated Carbon," *J. Chem. Eng. Jpn.*, **11**, 209 (1978).
Pierce, C., and B. Ewing, "Localised Adsorption on Graphite Surface," *J. Phys. Chem.*, **71**, 3408 (1967).
Quiggle, D., and M. Fenske, "Vapor-Liquid Equilibria of Methyl-Cyclohexane-Toluene Mixtures," *J. Amer. Chem. Soc.*, **59**, 1829 (1937).
Rao, M., and S. Sircar, "Thermodynamic Consistency for Binary Gas Adsorption Equilibria," *Langmuir*, **15**, 7258 (1999).
Reich, R., W. Ziegler, and K. Rogers, "Adsorption of Methane, Ethane, and Ethylene Gases and Their Binary and Ternary Mixtures and Carbon Dioxide on Activated Carbon at 212–301 K and Pressures to 35 Atmospheres," *Ind. Eng. Chem. Process. Des. Dev.*, **19**, 336 (1980).
Richter, E., W. Schutz, and A. Myers, "Effect of Adsorption Equation on Prediction of Multicomponent Adsorption Equilibria by the Ideal Adsorbed Solution Theory," *Chem. Eng. Sci.*, **44**, 1609 (1989).
Rudisill, E., and M. D. LeVan, "Multicomponent Adsorption Equilibrium: Henry's Law Limit for Pore Filling Models," **34**, 2080 (1988).
Russell, B., and M. D. LeVan, "Group-Contribution Theory for Adsorption of Gas Mixtures on Solid Surfaces," *Chem. Eng. Sci.*, **51**, 41025 (1996).
Ruthven, D. M., *Principles of Adsorption and Adsorption Processes*, Wiley, New York (1984).
Ruthven, D., and F. Wong, "Generalised Statistical Model for the Prediction of Binary Adsorption Equilibria in Zeolites," *Ind. Eng. Chem. Fundam.*, **24**, 27 (1985).
Sandler, S., *Chemical and Engineering Thermodynamics*, Wiley, New York (1999).
Sircar, S., "Excess Properties and Thermodynamics of Multicomponent Gas Adsorption," *J. Chem. Soc. Faraday Trans.*, **81**, 1527 (1985).
Sircar, S., "Role of Adsorbent Heterogeneity on Mixed Gas Adsorption," *Ind. Eng. Chem. Res.*, **30**, 1032 (1991a).
Sircar, S., "Isosteric Heats of Multicomponent Gas Adsorption on Heterogeneous Adsorbents," *Langmuir*, **7**, 3065 (1991b).
Sircar, S., "Influence of Adsorbate Size and Adsorbent Heterogeneity on IAST," *AIChE J.*, **41**, 1135 (1995).
Sircar, S., and A. Myers, "Surface Potential Theory of Multilayer Adsorption from Gas Mixtures," *Chem. Eng. Sci.*, **28**, 489 (1973).
Shapiro, A., and E. Stenby, "Potential Theory of Multicomponent Adsorption," *J. Colloid Int. Sci.*, **201**, 146 (1998).
Staudt, R., F. Dreisbach, and J. Keller, "Generalised Isotherms for Mono- and Multicomponent Adsorption," *Fundamentals of Adsorption*, M. D. LeVan, ed., Kluwer, Boston (1996).
Staudt, R., F. Dreisbach, and J. U. Keller, "Correlation and Calculation of Multicomponent Adsorption Equilibria Data Using a Generalized Adsorption Isotherm," *Adsorption*, **4**, 57 (1998).
Sundaram, N., "Equation for Adsorption from Gas Mixtures," *Langmuir*, **11**, 3223 (1995).
Suwanayuen, S., and R. Danner, "Vacancy Solution Theory of Adsorption from Gas Mixtures," *AIChE J.*, **26**, 76 (1980).
Talu, O., and R. L. Kabel, "Isosteric Heat of Adsorption and the Vacancy Solution Model," *AIChE J.*, **33**, 510 (1987).
Talu, O., and A. Myers, "Rigorous Thermodynamic Treatment of Gas Adsorption," *AIChE J.*, **34**, 1887 (1988a).
Talu, O., and A. Myers, Letter to the Editor, *AIChE J.*, **34**, 1931 (1988b).
Talu, O., and I. Zwiebel, "Multicomponent Adsorption Equilibria of Nonideal Mixtures," *AIChE J.*, **32**, 1263 (1986).
Tien, C., "Incorporation of the IAS Theory in Multicomponent Adsorption Calculations," *Chem. Eng. Commun.*, **40**, 265 (1986).
Valenzuela, D., A. Myers, O. Talu, and I. Zwiebel, "Adsorption of Gas Mixtures: Effect of Energetic Heterogeneity," *AIChE J.*, **34**, 397 (1988).
Xie, Z., K. Guo, J. Wu, and C. Yuan, "Adsorption Equilibrium of Vapor Mixture on Activated Carbon," *Fundamentals of Adsorption*, F. Meunier, ed., Elsevier, Paris (1998).
Yang, R. T., *Gas Adsorption by Adsorption Processes*, Butterworth, Boston (1987).
Yu, J. W., and I. Neretnieks, "Single Component and Multicomponent Adsorption Equilibria on Activated Carbon of Methylcyclohexane, Toluene and Isobutyl Methyl Ketone," *Ind. Eng. Chem. Res.*, **29**, 220 (1990).
Yun, J., H. Park, and H. Moon, "Multicomponent Adsorption Calculations Based on Adsorbed Solution Theory," *Korean J. Chem. Eng.*, **13**, 246 (1996).
Zheng, Y., and T. Gu, "Modified van der Waals Equation for the Prediction of Multicomponent Isotherms," *J. Colloid Int. Sci.*, **206**, 457 (1998).
Zhou, C., F. Hall, K. Gasem, and R. Robinson, "Predicting Gas Adsorption Using Two Dimensional Equations of States," *Ind. Eng. Chem. Res.*, **33**, 1280 (1994).

Appendix A: Vapor–Liquid Equilibria of Pure Substance

For the vapor–liquid equilibrium of a pure substance, the equilibrium is taken to be the equality between the rate of condensation and the rate of evaporation.

The rate of condensation of molecule A onto an interfacial liquid–vapor surface from a gas phase with a vapor pressure of p_A^0 is

$$k_A S p_A^0$$

while the evaporation rate from the same area is

$$k_{d,A} S \exp\left[-\frac{\lambda_A}{RT}\right]$$

where λ_A is the heat of vaporization. At equilibrium we get

$$\frac{k_{d,A}}{k_A} = p_A^0 \exp\left[\frac{\lambda_A}{RT}\right] \tag{A1}$$

This means that the ratio of the two rate constants is proportional to the vapor pressure and an exponential term involving the heat of vaporization.

Similarly, the vapor–liquid equilibrium of the pure substance B gives the following equation

$$\frac{k_{d,B}}{k_B} = p_B^0 \exp\left[\frac{\lambda_B}{RT}\right] \tag{A2}$$

Appendix B: Vapor–Liquid Equilibria of Binary Mixtures

In the case of binary mixtures, the equilibria are the same as those for pure substances, that is, the rate of condensation of a species from the vapor phase is the same as the rate of evaporation of the same species from the liquid phase.

The rate of condensation of molecule A onto an interfacial liquid–vapor surface from a gas phase having a pressure of p_A is

$$k_A^{(\text{mixture})} S p_A$$

where the superscript *mixture* means that the rate constant is that for mixture, to distinguish it from the rate constant for pure substance, k_A, which is defined in Appendix A.

Since the mole fraction of A in the liquid is x_A, the rate of evaporation of A from the same area S is

$$k_{d,A}^{(\text{mixture})} S x_A \exp\left[-\frac{Q_A(x_A, x_B)}{RT}\right]$$

where $Q_A(x_A, x_B)$ is the heat required to desorb one mole of species A from a liquid mixture having compositions of x_A and x_B. Equating the preceding two rates, we get

$$\frac{k_{d,A}^{(\text{mixture})}}{k_A^{(\text{mixture})}} = \frac{p_A}{x_A} \exp\left[\frac{Q_A(x_A, x_B)}{RT}\right] \tag{B1}$$

If we assume that the ratio of the rate constants for A in the mixture is the same as that for pure A, we can equate Eqs. A1 and B1 to get

$$\exp\left[\frac{Q_A(x_A, x_B) - \lambda_A}{RT}\right] = \frac{p_A^0 x_A}{p_A} \tag{B2}$$

Doing the same for the species B, we obtain a similar equation for B, as given below

$$\exp\left[\frac{Q_B(x_A, x_B) - \lambda_B}{RT}\right] = \frac{p_B^0 x_B}{p_B} \tag{B3}$$

In general, the LHS of Eqs. B2 and B3 is a function of mole fraction x_A. The special case is that when they are equal to unity, Raoult's law is the result.

If the experimental data of vapor–liquid equilibrium for mixture are available or calculated from the PR EOS, we can evaluate the RHS of Eqs. B2 and B3. Hence, we define

$$f_A(x_A) = \exp\left[\frac{Q_A(x_A, x_B) - \lambda_A}{RT}\right] \tag{B4}$$

$$f_B(x_A) = \exp\left[\frac{Q_B(x_A, x_B) - \lambda_B}{RT}\right] \tag{B5}$$

and they are defined functions of the mole fraction. This allows us to estimate the heats of evaporation of A and B from a liquid mixture that has composition of (x_A, x_B).

Appendix C: Calculation of Vapor–Liquid Equilibria with Peng-Robinson Equation of State

The Peng–Robinson equation is one of the most celebrated cubic equations of state to describe the state of vapor–liquid for both pure substances and for mixtures. The Peng–Robinson equation for mixture is written as (Sandler, 1999)

$$P = \frac{RT}{V-b} - \frac{a(T)}{V(V+b)+b(V-b)} \tag{C1}$$

where P is the total pressure (Pa), T is the absolute temperature (K), V is the molar volume of the mixture, and a and b are parameters for the mixture. The parameters a and b are calculated from the corresponding parameters of pure substances

$$a = \sum_{i=1}^{n} \sum_{j=1}^{n} y_i y_j a_{ij} \tag{C2a}$$

$$b = \sum_{i=1}^{n} y_i b_i \tag{C2b}$$

$$a_{ij} = \sqrt{a_i a_j}\,(1 - k_{ij}) \tag{C2c}$$

where k_{ij} is the binary interaction parameter.

The pure substance parameters a_i and b_i are calculated from the critical properties of that substance and the acentric parameter ω

$$a_i(T) = 0.45724 \frac{R^2 T_{c,i}^2}{P_{c,i}} \alpha_i(T) \tag{C3a}$$

$$b_i = 0.07780 \frac{RT_{c,i}}{P_{c,i}} \tag{C3b}$$

$$\sqrt{\alpha_i} = 1 + \kappa_i\left(1 - \sqrt{\frac{T}{T_{c,i}}}\right) \tag{C3c}$$

$$\kappa_i = 0.37464 + 1.5226\,\omega_i - 0.26992\,\omega_i^2 \tag{C3d}$$

Another derivative of the PR equation is the PR-SV suggested by Stryjek and Vera, who introduced a specific parameter κ_1 for the substance involved. For this model, the parameter κ_i in Eq. C3d is replaced by

$$\kappa_i = 0.378893 + 1.4897153\,\omega + 0.17131848\,\omega_i^2 + 0.0196554\,\omega_i^3 + \kappa_1\left(1 + \sqrt{\frac{T}{T_c}}\right)\left(0.7 - \frac{T}{T_c}\right) \tag{C3e}$$

From the PR EOS for mixture, the fugacity for either the liquid phase or the gas phase can be calculated from

$$\ln\left[\frac{\bar{f}_i(T, P, \underline{y})}{Py_i}\right] = \frac{B_i}{B}(Z-1) - \ln(Z-B) - \frac{A}{2\sqrt{2}\,B}\left[\frac{2\sum_j y_j A_{ij}}{A} - \frac{B_i}{B}\right] \ln\left[\frac{Z + (1+\sqrt{2})\,B}{Z + (1-\sqrt{2})\,B}\right] \tag{C4}$$

where

$$A = \frac{aP}{(RT)^2}; \qquad B = \frac{bP}{RT}; \qquad A_{ij} = \frac{a_{ij}P}{(RT)^2}; \qquad B_i = \frac{b_iP}{RT} \tag{C5}$$

and Z is the root of the following cubic equation

$$Z^3 - (1-B)Z^2 + (A - 3B^2 - 2B)Z - (AB - B^2 - B^3) = 0 \tag{C6}$$

For the vapor phase, use the low value of Z, and for the liquid phase, use the high value of Z.

The condition for calculating equilibrium between vapor and liquid of mixtures is the equality of fugacities of the two phases

$$f_i^{-L}(T, P, \boldsymbol{x}) = \tilde{f}_i^{V}(T, P, \boldsymbol{y}) \tag{C7}$$

Manuscript received April 3, 2001, and revision received Mar. 11, 2002.